Wind-Induced Barotropic Motions in Long Lakes[1]

G. T. CSANADY[2]

Woods Hole Oceanographic Institution, Woods Hole, Mass. 02543

(Manuscript received 22 March 1973, in revised form 27 April 1973)

ABSTRACT

Water motion in the barotropic mode, directly forced by suddenly imposed wind stress, is investigated in basins with arbitrary topography, but paying special attention to long basins, in which the depth contours run parallel to the shores over a "trunk" region. In the initial period the depth-integrated transport is found to increase linearly in time; later, friction slows down this increase. Where the water is shallower than the average depth of the lake, transport is with the wind; it is against the wind in the deeper portion. Over the entire basin, a transport-streamline pattern may be calculated numerically, which is identical in appearance with the steady-state flow pattern calculated on the basis of assuming bottom friction to be linearly related to transport. A more realistic frictional force (quadratic in the velocity) modifies this pattern somewhat, but does not change it qualitatively.

An analysis of IFYGL coastal chain observations in Lake Ontario shows that the observed nearshore transport behaves much as the theoretically derived forced flow pattern. One may conclude that in nearshore areas (for practical purposes, in water shallower than the basin average depth), the forced component of the flow dominates the observable depth-integrated transport, oscillating movements (seiches) being relatively less important. This forced flow pattern may be described as consisting of barotropic coastal jets.

1. Introduction

The more intensive studies of water movements in the North American Great Lakes carried out in recent years [and especially the International Field Year (IFYGL), a just completed detailed study of Lake Ontario] have demonstrated with considerable force that the major prime movers of currents are short bursts of strong winds. Not that this should have come as a surprise: winds are known to be quite variable at these latitudes and to attain gale force on occasion. The stress of the wind over water is known to be a quadratic function of wind speed, a fact which accentuates greatly the importance of storms.

Because strong wind stress impulses are exerted on the water at random times, at a typical frequency of about once in 100 hr, and because the strength and direction of these impulses vary in a random manner, water movements produced by them are always essentially in a transient state, there being never enough time to obtain any sort of a steady-state flow pattern. It is quite possible that some residual, long-term average circulation still exists, but the intensity of this is certain to be much less than that of the transient patterns. Therefore, in order to understand the first-order dynamics of the observable water movements, it is necessary to study time-dependent theoretical models.

One theoretical problem in this category is the response of a long and narrow lake of homogeneous density to a suddenly applied wind stress. One may easily gain the over-optimistic impression from the literature that the basic physical factors involved in this problem are well understood: the wind is supposed to cause a static "set-up" or accumulation of water at the downwind end, and to start off several modes of free oscillations (seiches). While the art of numerical modeling of such phenomena in basins of complex shape is advanced [witness the study of the North Sea storm surge problem by Heaps (1969), or of the Lake Ontario winter circulation by Paskausky (1971)], such numerical calculations often yield results whose physical meaning is just as difficult to decipher as observed phenomena. The *aperiodic* part of the barotropic response to wind stress in realistic lake models has still not been studied with the aid of theoretical models of sufficient simplicity to exhibit the basic dynamical factors involved. In a nonrotating basin of constant depth, the aperiodic or forced response is a simple surface distortion (set-up), a constant non-zero surface slope balancing the wind stress. In a basin of variable depth the set-up is accompanied by a non-trivial forced flow pattern, as will be seen below.

The present paper is devoted to a study of the wind-forced flow problem in basins of variable depth, but especially in lakes which are much longer than they are wide, and which are also narrow enough for the rotation of the earth not to affect barotropic motions very significantly. The "trunk" region of such lakes will be assumed to have parallel shores and depth contours. Such a theoretical model bears close resemblance to Lake Ontario, the bathymetry of which is

[1] Contribution No. 3082, Woods Hole Oceanographic Institution.

[2] On leave from University of Waterloo, Ontario.

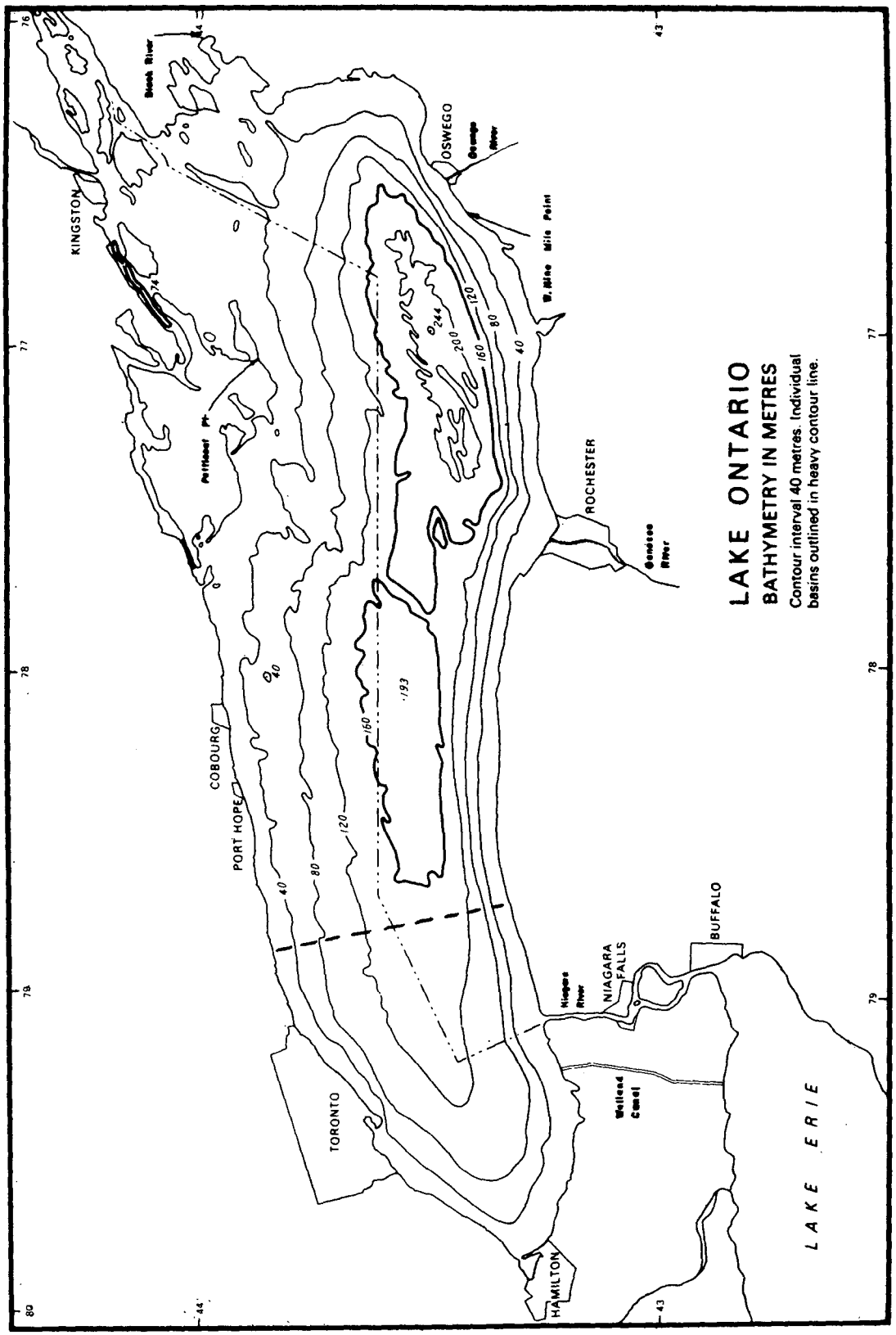

FIG. 1. Depth contours in Lake Ontario, after Sweers (1969). Oshawa-Olcott cross section is shown by dashed line east of Toronto.

shown in Fig. 1. The theoretical conclusions are compared with current observations at coastal chains, which were carried out in Lake Ontario during IFYGL.

2. Formulation of the problem

Consider at first a basin of arbitrary shape and depth distribution, over which a wind stress constant in time (but arbitrarily distributed in the horizontal plane) is imposed suddenly at $t=0$. We neglect the Coriolis forces for the time being and write the depth-integrated equations of motion and continuity for the volume transport components U, V, linearized, and with the hydrostatic approximation assumed, as follows:

$$\left.\begin{aligned} \frac{\partial U}{\partial t} &= -gh\frac{\partial \zeta}{\partial x}+F_x \\ \frac{\partial V}{\partial t} &= -gh\frac{\partial \zeta}{\partial y}+F_y \\ \frac{\partial U}{\partial x}+\frac{\partial V}{\partial y} &= -\frac{\partial \zeta}{\partial t} \end{aligned}\right\}, \tag{1}$$

where F_x, F_y are the components of the wind stress divided by density, $h(x,y)$ the water depth, and ζ the surface elevation from equilibrium. The linearization does not apply in the immediate vicinity of the shores where $h \to 0$, but in dealing with relatively large-scale motions this complication may be safely ignored. However, the absence of bottom friction terms in Eqs. (1) is only justifiable in the initial period of response, before significant velocities develop. At later times F_{bx}, F_{by} have to be added to the right-hand sides of the first and second of Eqs. (1).

In common with many other oscillating systems, the response of the lake to a suddenly applied wind stress consists of a directly forced motion [mathematically, a particular solution of Eqs. (1)] and of a sequence of free oscillations known as "seiches" (homogeneous solutions), whose amplitudes are proportional to the stress and depend on basin geometry. While there is an almost overwhelming wealth of literature on seiches [for a recent review see Wilson (1972)], mostly dealing with the calculation of natural frequencies for an impressive range of geometries, little or no attention seems to have been paid to the forced solution. We shall therefore concentrate on the latter, ignoring the well-explored seiche problem.

The only forced solution of Eqs. (1) which has apparently ever been discussed is that valid for a constant depth basin ($h=$constant) and for spatially constant wind stress. The simplicity of the result is perhaps the reason for the uniform neglect of the forced motion problem:

$$\zeta=\frac{F_x}{gh}x+\frac{F_y}{gh}y, \quad U=0, \quad V=0, \tag{2}$$

where the origin of the coordinate axes are at the centroid of the lake surface. This solution is referred to as a static set-up of the lake. It is at once obvious that (2) does not satisfy (1) for $h(x,y)\neq$constant.

For a more realistic depth distribution we may still hope to find a time-independent elevation distribution (i.e., a somewhat more complicated set-up) $\zeta(x,y)$, so that $\partial\zeta/\partial t=0$. The structure of Eqs. (1) then suggests that U and V should be linear functions of time, i.e.,

$$U=At, \quad V=Bt. \tag{3}$$

Substituting into Eqs. (1), we find

$$\left.\begin{aligned} A &= -gh\frac{\partial \zeta}{\partial x}+F_x \\ B &= -gh\frac{\partial \zeta}{\partial y}+F_y \\ \frac{\partial A}{\partial x}+\frac{\partial B}{\partial y} &= 0 \end{aligned}\right\}. \tag{4}$$

The boundary conditions are that the normal components of the transport vanish at the shores at all times t, so that the same condition applies to the accelerations A, B. If, subject to these conditions, Eqs. (4) may be solved, the solution yields a time-independent surface level distribution accompanied by a non-trivial transport distribution, increasing linearly with time.

It is not difficult to demonstrate that such solutions may, in fact, be found. The third of Eqs. (4) may be satisfied by introducing a streamfunction for the accelerations:

$$A=\frac{\partial \Psi}{\partial y}, \quad B=-\frac{\partial \Psi}{\partial x}. \tag{5}$$

The boundary condition at the shores is now $\Psi=$constant, a streamline coinciding with the coastline. Eliminating ζ from the first two of Eqs. (4), we find

$$\frac{\partial}{\partial x}\left[\frac{1}{gh}\left(\frac{\partial \Psi}{\partial x}-F_y\right)\right]+\frac{\partial}{\partial y}\left[\frac{1}{gh}\left(\frac{\partial \Psi}{\partial y}-F_x\right)\right]=0. \tag{6}$$

This equation may be integrated (e.g., numerically). For Lake Ontario, Rao and Murthy (1970) have presented such numerical solutions for different wind stress distributions, although they placed a different physical interpretation on their results (see later discussion). Their solutions were calculated for the actual, irregular topography of this Lake, only slightly smoothed to facilitate the numerical work. Similar solutions may clearly be found for other arbitrarily shaped closed basins: we may legitimately regard these as the forced responses of a lake to a given wind stress, for vanishing friction and Coriolis force.

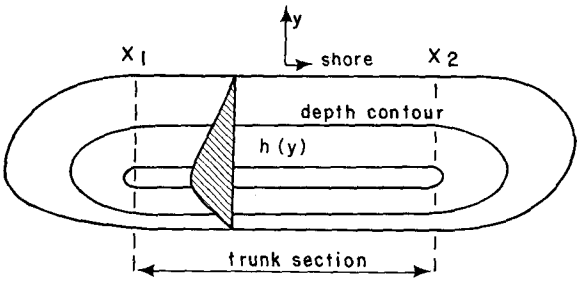

FIG. 2. Schematic diagram of long and narrow lake with regular trunk section, in which depth contours are parallel.

3. The special case of long lakes

Relatively simple results are obtained in long lakes which contain a considerable trunk region with parallel shores and depth contours. An idealized model of such a lake is sketched in Fig. 2. This represents reasonably realistically a number of long lakes, and in particular Lake Ontario. The lake is taken to be much longer than it is wide. We place the x-axis along the length of the lake and consider the forced motion produced by a constant (in space and time) wind stress acting along this same axis ($F_x=F=$constant, $F_y=0$). With an eye on interpreting field observations, we seek to determine the transport distribution in a cross section ($x=$constant plane) within the trunk region.

At *any* cross section (whether in the trunk region or not) we have on integrating the third of Eqs. (4) over a region to *one side* of the cross section, by the divergence theorem and in virtue of the boundary conditions:

$$\int_{y_1}^{y_2} A\,dy=0, \tag{7}$$

where y_1 and y_2 are the coordinates of the shores. In the trunk region, $x_1<x<x_2$, we expect any transport to be parallel to the boundaries and depth contours, i.e.,

$$\left.\begin{aligned} B&=0\\ A&=-gh\frac{d\zeta}{dx}+F, \quad x_1\leqslant x\leqslant x_2 \end{aligned}\right\}. \tag{8}$$

Imposing the condition expressed by Eq. (7), we find the elevation gradient

$$\frac{d\zeta}{dx}=\frac{Fb}{gS}, \quad x_1<x<x_2, \tag{9}$$

where $b=y_2-y_1$ is the width of the lake and S is its cross-sectional area:

$$S=\int_{y_1}^{y_2} h\,dy. \tag{10}$$

Returning to Eqs. (8) and (3), we may now write the transport in the trunk region as

$$U=Ft\left(1-\frac{hb}{S}\right), \quad x_1<x<x_2. \tag{11}$$

It may be verified directly that Eqs. (9) and (11) constitute a solution of Eqs. (1) for the trunk region of the lake.

The simple relationship in Eq. (11) is illustrated in Fig. 3, using the depth distribution of Lake Ontario south of Coburg as an example. The transport distribution is clearly a rescaled and displaced depth distribution. The calculated transport is zero where $h=S/b$, which is the *average* depth of the section. The elevation gradient $d\zeta/dx$ may be seen to be the same as would be produced in a lake of this average depth [Eq. (9)]. Given this depth, the wind stress and the pressure gradient are in balance. Where the depth is less, the wind stress overwhelms the pressure gradient and

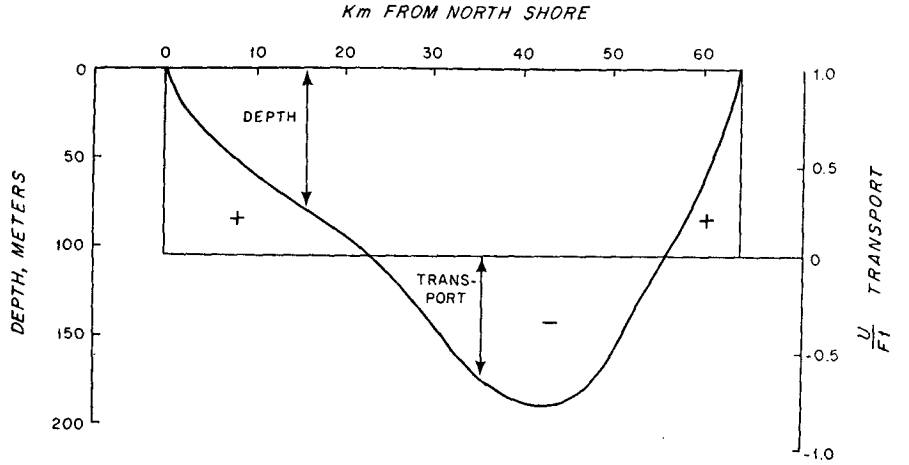

FIG. 3. Distribution of depth and theoretically derived transport, using Lake Ontario as an example.

accelerates the water. Where the water is deeper, the reverse happens and a return flow develops.

The transport distribution in the remainder of the basin may now also be elucidated qualitatively with very little difficulty. Recalling that by Eqs. (5) and (6) the A, B distribution may be represented by a streamline pattern, we can draw the streamlines in the trunk region with the correct spacing to correspond to the calculated transport pattern. This yields relatively densely spaced lines both at the center and at the shores, pointing in opposite directions, however. In the end regions these streamlines must close: the details depend on the depth distribution, but the appearance of a "double-gyre" pattern follows regardless of these details, much as sketched in Fig. 4 in which a not too irregular basin was tacitly assumed. Fig. 5 shows the calculated pattern for constant wind stress slong the longer axis of Lake Ontario (Rao and Murthy, 1970), which is not quite so symmetrical, but agrees with the qualitative inference from the simplified theory for a parallel trunk region. The gyres are indeed related to the actual depth distribution. It is also of interest to calculate the velocities $u = U/h$ for the trunk region, given a realistic wind impulse, say $Ft = 20{,}000$ cm^2 sec^{-1} (a stress of 1 dyn cm^{-2} acting for about 6 hr); these are shown in Fig. 6. Near the shores a singularity occurs on account of the depth h reducing to zero. In very shallow water it is not realistic to neglect friction even for a short initial period: observable velocities at short times would presumably behave somewhat like the conjectured dotted curve in Fig. 6. Note also that if some transport is suppressed near the shores, the center return flow is similarly diminished. Frictional effects are considered in greater detail later.

The velocity distribution is noteworthy in that it shows the development of strong barotropic coastal currents. Although the mechanism of these differs from that of the baroclinic coastal jets described earlier (Csanady, 1972a), the net practical effect is much the same, i.e., bands of high velocity occurring in the coastal zone.

For the practical application of these results one must keep in mind that the above forced flow pattern is accompanied by seiches. The amplitude of seiche currents is (for the typical wind stress assumed above) of

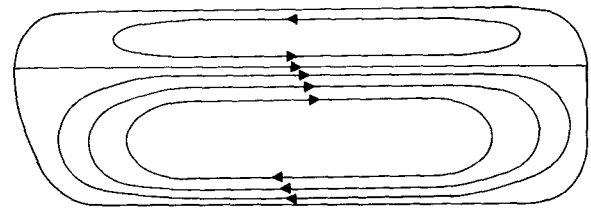

FIG. 4. General appearance of wind-forced transport streamlines in long and narrow lakes.

the order of 1 cm sec^{-1}, uniform over the cross section, and initially these are directed downwind. Thus, the combination of seiche current and forced flow pattern results in near-zero velocities in the center part of a lake (where the two initially more or less cancel each other) and a slightly fortified barotropic coastal current as compared to the distribution in Fig. 6.

Barotropic coastal jets of this sort have first been identified by Bennett (1972) in connection with analytical and numerical studies of an idealized shore zone. Some of Bennett's assumptions in the analytical part of his work may be thought contentious. For example, Bennett postulates the equivalent of our Eq. (7) essentially without justification, while also retaining the Coriolis force in his theory. It will be seen below that these assumptions are incompatible. The same objections do not apply to Bennett's numerical studies, which show nearshore flow patterns much as found above with the aid of an analytical model. Bennett also invokes the "rigid lid approximation," perhaps unnecessarily. It should be noticed that our approach is in no way equivalent to the rigid lid approximation: we have merely been looking for (and found) a forced flow pattern accompanied by a time-independent, free surface elevation distribution.

That barotropic coastal jets at a typical velocity amplitude (much as shown in Fig. 6) in fact frequently occur in Lake Ontario was shown by the results of the "coastal jet" project (Csanady and Pade, 1969–72). Birchfield (1972) drew attention to this fact, and proposed a theoretical explanation in terms of a frictionally dominated, steady-state flow pattern. However, it is clear that the observed jets were not in any kind of steady state, and the above explanation, as barotropic forced response, appears much more realistic.

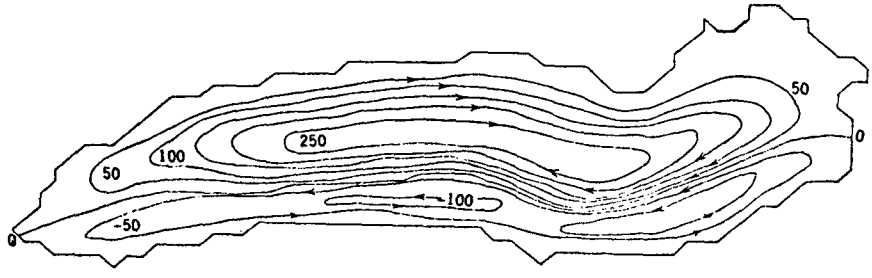

FIG. 5. Calculated pattern of wind-forced transport streamlines for Lake Ontario. After Rao and Murthy (1970).

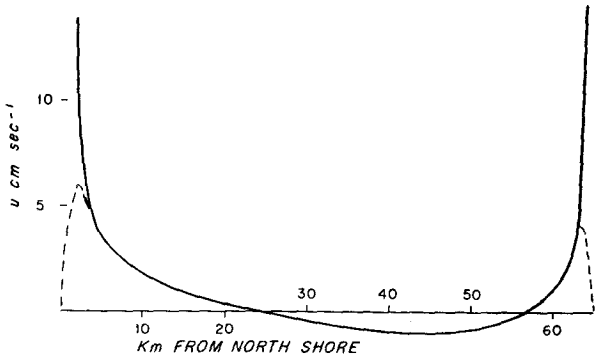

FIG. 6. Velocity distribution corresponding to the transport distribution in Fig. 3.

4. Effect of the Coriolis force

Should the Coriolis force due to the rotation of the earth become important in this problem, the terms $-fV$, fU respectively would have to be included on the left-hand side of the first and second of Eqs. (1). Focussing on the *trunk* region of a long lake only, a forced solution of the so expanded equations may be found in the form

$$\left.\begin{aligned} U&=At, & V&=V(y)\neq 0\\ \frac{\partial\zeta}{\partial x}&=G=\text{constant}, & \frac{\partial\zeta}{\partial y}&=Zt\neq 0 \end{aligned}\right\}, \tag{12}$$

where $Z=Z(y)$. On substitution into the expanded Eqs. (1), one arrives at the relationships

$$\left.\begin{aligned} A-fV&=-ghG+F\\ fA&=-ghZ\\ \frac{d^2V}{dy^2}&=-Z \end{aligned}\right\}, \tag{13}$$

for $x_1<x<x_2$.

These equations are somewhat more complicated counterparts of Eq. (8) and may be solved for given $h(y)$, subject to the boundary conditions $V=0$ at y_1, y_2. Very similar equations govern the development of internal mode (baroclinic) coastal jets along an "infinite" shore or continental shelf (Csanady, 1973), the only difference being in the forcing term, which also becomes depth-dependent.

Because the surface elevation now also depends on time, Eq. (7) no longer follows from the equation of continuity. Indeed, the full solution of the initial value problem for very simple topography (Csanady, 1972a) shows that the coastal jets supply a certain volume of water from the upwind to the downwind end of the basin, which leads to a slow propagation of the flow pattern around the basin perimeter in a counterclockwise direction (in the Northern Hemisphere), in the form of a Kelvin-type wave. From Eqs. (13), on two partial integrations, and noting that at the shores both h and V are zero, one may show that

$$\int_{y_1}^{y_2} A\,dy=\frac{g}{f}\int_{y_1}^{y_2}\frac{d^2h}{dy^2}V\,dy. \tag{14}$$

The effect of the Coriolis force is to produce a drift to the right of the wind stress, i.e., a negative V for positive F. The basin bottom is generally speaking concave, i.e., d^2h/dy^2 negative. Thus a positive value of the integral in Eq. (14) results for positive wind stress.

The case with Coriolis force differs from the previously discussed no-rotation case mainly to the extent that fV is not negligible compared to A in the first of Eqs. (13). If the maximum value of V occurs at $y=y_c$ (so that dV/dy is zero there) we may express V from the second and third of Eqs. (13) as

$$V=\int_0^y\int_{y_c}^{y^1}\frac{fA}{gh}dy^{11}dy^1. \tag{15}$$

If A_m is the maximum value of A in the cross section, and V_m that of V, we therefore have the inequality

$$\left|\frac{fV_m}{A_m}\right|\leq\left|\frac{f^2}{g}\int_0^{y_c}\int_{y_c}^{y^1}\frac{dy^{11}}{h}dy^1\right|. \tag{16}$$

Because the lake bottom is concave, the inequality is true *a fortiori* if we replace h in the integrand by h_cy/y_c, where h_c is the lake depth at $y=y_c$. The integrations may then be carried out and yield

$$\left|\frac{fV_m}{A_m}\right|<\frac{f^2y_c^2}{gh_c}. \tag{17}$$

The result shows that the Coriolis acceleration is negligible in comparison with the local acceleration if y_c is small compared to the radius of deformation $(gh_c)^{\frac{1}{2}}/f$. For a symmetrical basin y_c would be equal to half the basin width b, and h_c to the maximum basin depth. While Lake Ontario is not quite symmetrical, $h_c=150$ m and $y_c=30$ km are reasonable values to use in the above estimate, leading to

$$\left|\frac{fV_m}{A_m}\right|<6\times10^{-3},$$

which is indeed suitably small.

This result would encourage one to regard rotational effects minor in the barotropic forced motion problem in a lake of the width of Lake Ontario. However, a disturbing point is that the longshore pressure gradient may differ significantly from the value calculated in Eq. (9). From the first of Eqs. (13) and from (14), one finds

$$-gGS+Fb=\int_{y_1}^{y_2}\left(\frac{g}{f}\frac{d^2h}{dy^2}-f\right)dy. \tag{18}$$

The second derivative d^2h/dy^2 is of order h_c/y_c^2; for a symmetrical, parabolic depth distribution it is constant, equal to $2h_c/y_c^2$, where $y_c=b/2$ and h_c is the center depth. Therefore, the first term in the integral in (18) is large compared to the second, this ratio being exactly twice the reciprocal of the right-hand side of Eq. (17). Thus the right-hand side of (18) is of order $A_m b$, which is of order Fb; hence, Eq. (9) is replaced by

$$\frac{d\zeta}{dx}=G=\gamma\frac{Fb}{gS}, \tag{19}$$

where

$$\gamma=1-\frac{g}{fFb}\int_{y_1}^{y_2}\frac{d^2h}{dy^2}V\,dy,$$

and $(1-\gamma)$ is of order unity. This change mainly affects the flow in the center portion of the cross section where the pressure gradient dominates. Near the shores, where the wind stress dominates, the change is not likely to be of much practical importance. Nevertheless, it is interesting to note that the Coriolis force makes the longshore pressure gradient dependent on conditions outside the trunk region, in the end regions of the basin. For an infinitely long channel one would postulate $\gamma=0$: this is indeed the basis of idealized coastal jet calculations in the baroclinic mode (Csanady, 1973), in which case the actual basin length is in fact very large compared to the (internal) radius of deformation. At the other extreme, one would intuitively expect Eq. (9) to remain satisfied for sufficiently short lakes. It is not clear from the present simplified theory exactly at what length to radius of deformation ratio the longshore pressure gradient would begin to diminish significantly.

5. Effect of friction

If the wind blew with constant force for a very long time, the linear increase in transport would certainly be reduced by bottom friction. After a long time a steady-state flow pattern would indeed be established. Although it is unlikely that such a steady state would ever be reached in a lake at mid-latitudes, the asymptotic flow pattern is still of interest as possibly illustrating what the tendency of any changes would be, from the initial pattern we have already discussed.

We therefore return to Eqs. (1), set the time-dependent terms all zero and introduce bottom friction terms on the right. Although such friction is in fact quadratic in velocities, a frequently used simplification is to assume *linear* friction:

$$F_{bx}=-kU,\quad F_{by}=-dV, \tag{20}$$

where k is effectively a transport "decay constant," a reciprocal of the time scale in which a given flow pattern would die away.

Making this substitution, Eqs. (1) become

$$\left.\begin{aligned} kU&=-gh\frac{\partial\zeta}{\partial x}+F_x\\ kV&=-gh\frac{\partial\zeta}{\partial y}+F_y\\ \frac{\partial V}{\partial x}&+\frac{\partial U}{\partial y}=0 \end{aligned}\right\}. \tag{21}$$

The boundary conditions are again that the transport vanishes normal to the boundary (we have included no lateral friction). Eqs. (21) and the boundary conditions are clearly identical to Eqs. (4), if we replace A, B by kU, kV. Therefore, the calculated acceleration-streamline pattern is at once the asymptotic steady-flow streamline pattern. The calculations of Rao and Murthy (1970) were carried out to discover this steady-flow streamline pattern, using Eqs. (21) as the starting point.

It is easy to see now that at some intermediate time, when neither $\partial U/\partial t$ nor kU are negligible, Eqs. (1) with linear friction included yield for the *forced* part of the motion only (i.e., setting $\partial\zeta/\partial t=0$):

$$\left.\begin{aligned} \left(\frac{\partial}{\partial t}+k\right)U&=-gh\frac{\partial\zeta}{\partial x}+F_x\\ \left(\frac{\partial}{\partial t}+k\right)V&=-gh\frac{\partial\zeta}{\partial y}+F_y\\ \frac{\partial}{\partial x}\left[\left(\frac{\partial}{\partial t}+k\right)U\right]&+\frac{\partial}{\partial y}\left[\left(\frac{\partial}{\partial t}+k\right)V\right]=0 \end{aligned}\right\}. \tag{22}$$

These are again of the same form as Eqs. (4) so that the calculations of the streamline pattern still hold, if we replace A, B according to the scheme

$$\left.\begin{aligned} \left(\frac{\partial}{\partial t}+k\right)U&=A\\ \left(\frac{\partial}{\partial t}+k\right)V&=B \end{aligned}\right\}. \tag{23}$$

These are simple differential equations in time, and for zero initial transport have the solutions

$$\left.\begin{aligned} U&=\frac{A}{k}(1-e^{-kt})\\ V&=\frac{B}{k}(1-e^{-kt}) \end{aligned}\right\}. \tag{24}$$

At short times we recover the solution (U,V)

$=(At,Bt)$, while at long times (U,V) tend to $(A/k,B/k)$, the pattern remaining all along unchanged.

No such simple results are obtained with quadratic friction. The bottom friction along the x-axis is in this case

$$F_{bx}=-c_d\frac{U}{h}\left|\frac{U}{h}\right|, \tag{25}$$

where c_d is the drag coefficient. In the trunk section of a long, narrow lake we therefore have

$$c_d\left|\frac{U}{h}\right|\frac{U}{h}=F-gh\frac{d\zeta}{dx}, \tag{26}$$

which is subject to the condition, from the equation of continuity, that

$$\int_{y_1}^{y_2} U\,dy=0. \tag{27}$$

At some intermediate depth h_d the transport vanishes. At shallower depth, it is directed downwind; at $h>h_d$, upwind. The surface slope, from (26), is

$$\frac{d\zeta}{dx}=\frac{F}{gh_d}. \tag{28}$$

For a given depth distribution, h_d may be calculated from Eq. (27), and then the transport distribution determined.

The distribution of the depth-integrated longshore transport, calculated with quadratic friction in the manner described, for a cross section of Lake Ontario south of Coburg (using a drag coefficient of $c_d=2\times10^{-3}$) is shown in Fig. 7a. Corresponding velocities $u=U/h$ are shown in Fig. 7b. The barotropic coastal jet is still quite evident in the velocity distribution, although the contrast with mid-lake is much less pronounced. The transport-streamline pattern changes somewhat compared to the linear-friction calculation (Fig. 4), although not in a qualitative way. Because h_d is *greater* than the average depth, the asymptotic pressure gradient is less than the initial one [cf. Eq. (28)].

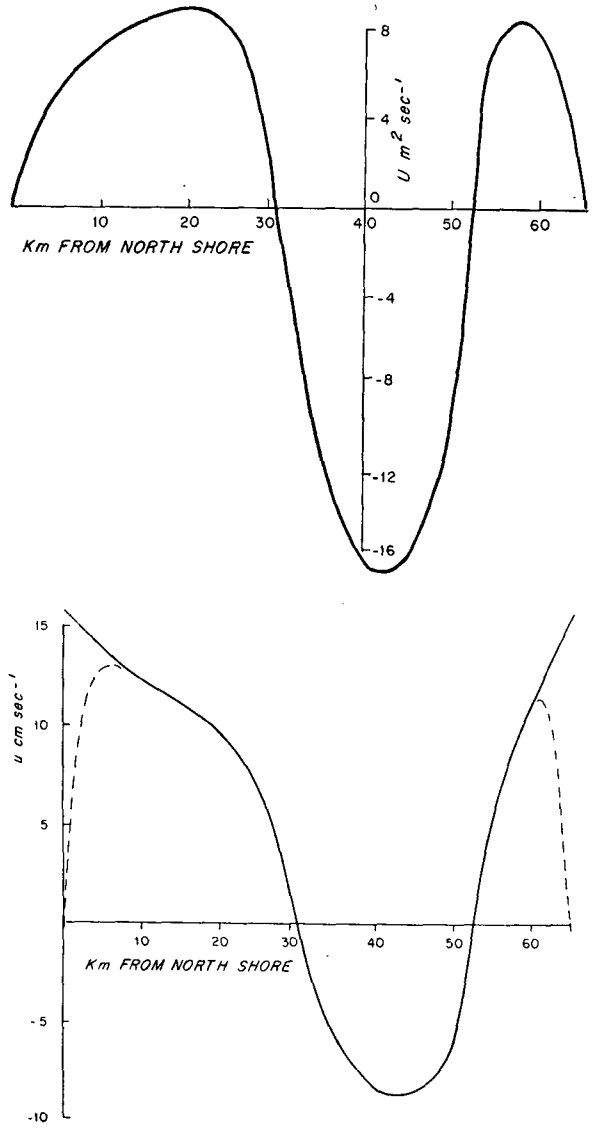

FIG. 7. Transport distribution with quadratic friction (a) and the corresponding velocity distribution (b) for the cross section in Fig. 3.

6. Comparison with IFYGL observations

The observations carried out during the International Field Year on Lake Ontario provide for the first time a sufficiently detailed set of data for testing theories of the above kind. The main sources of information for this purpose are the coastal chain studies, carried out by a technique previously described (Csanady, 1972b) at several locations both on the south and north shores. The coastal chain observations yielded the current velocity distributions in chosen cross sections, extending from the shores to 10–14 km into the lake. There was sufficient resolution to give reasonable estimates of depth-integrated transports and their distribution in the key nearshore bands. During well-defined storms the winds may be expected to be more or less uniform over the whole lake and the wind stress impulse estimated with acceptable accuracy from meteorological data. The observed response of the lake to such a wind stress impulse should show the characteristics predicted by the theory developed above.

Two clear-cut wind stress impulses occurred early in August 1972, during the second alert period of IFYGL. We shall focus here on the response of the lake during these episodes, as determined by the observations in the Olcott-Oshawa cross section, approximately 90 km east of the western tip of the lake, in a more or less regular trunk region (in the sense of the simple theory discussed before). The data of the Olcott chain, including calcu-

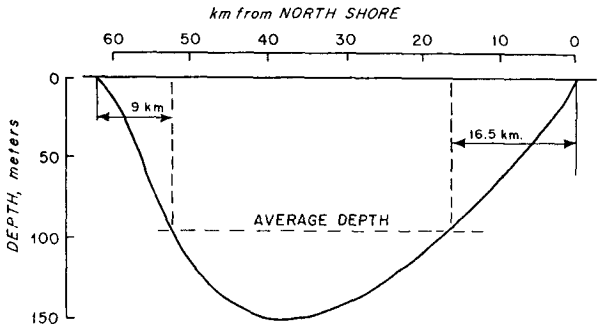

FIG. 8. Depth distribution in Lake Ontario along Olcott-Oshawa section.

lated depth-integrated transports, were kindly placed at my disposal by Dr. J. T. Scott of SUNY, Albany—the Oshawa data are our own.

The depth distribution of the lake in this section is shown in Fig. 8. Late on 6 August a 7-hr easterly blow took place, with hourly winds of up to 6 m sec^{-1}. The total estimated *westward* wind stress impulse for this storm was approximately

$$Ft = 25{,}000 \text{ cm}^2 \text{ sec}^{-1}.$$

Another, oppositely directed wind stress impulse was exerted on the water on 9 August, with hourly winds of up to 15 m sec^{-1}, lasting some 10 hr, and yielding a total estimated wind stress impulse of (again counting westward impulse as positive)

$$Ft = -90{,}000 \text{ cm}^2 \text{ sec}^{-1}.$$

Detailed current distributions during stormy weather could not always be determined but have been obtained at Oshawa on 8 and 10 August and at Olcott on 10 August. Depth-integrated transports in the shore-parallel direction, calculated from the observations, are shown in Figs. 9 and 10. The dotted line in Fig. 9 shows the change in transport from 8–10 August, presumably caused by the wind stress impulse on the 9th.

Except for fairly obvious effects of friction and some minor irregularities, the observations show a transport distribution very much as expected from theory. The maximum transports agree well in order of magnitude with the wind stress impulse estimate. The strongest support for the theory comes from the observation that the integrated transports tended to zero near the locus of the average depth both along the north and the south shores. The detailed theoretical transport distribution (for comparison with the data) may be taken to be the depth curve in Fig. 8, with the horizontal line labeled "average depth" as the abscissa, and the ordinate appropriately rescaled. The discrepancy between theory and observation is of course strong in very shallow water, for reasons already discussed. It is clear, however, that frictional influences are not nearly strong enough to eliminate the coastal jets predicted by frictionless theory. Indeed, coastal zone observations

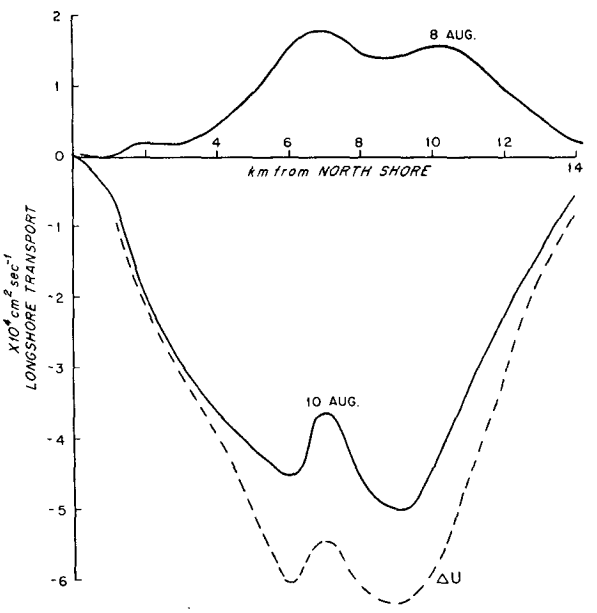

FIG. 9. Observed transport distribution along Oshawa coastal chain following two storm episodes during the second IFYGL alert.

seem to constitute a rather critical test of the theoretical arguments given above.

Accepting the basic correctness of the theory, one may infer to what distance from shore bottom friction

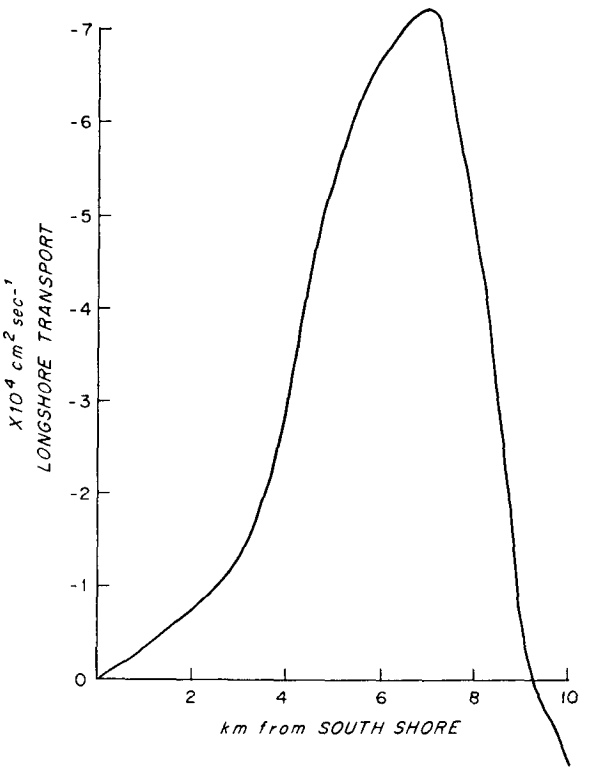

FIG. 10. Observed transports along Olcott coastal chain (data of J. T. Scott).

exerts a controlling influence on the transport. Frictionless theory yielded maximum transports at the shore (cf. Fig. 3). The observations showed maxima at 7–9 km. This may for practical purposes be regarded as the edge of a "frictional" coastal boundary layer. The depth of water at this distance was about 50 m.

7. Conclusions

We have shown that wind stress applied at the surface of a basin of variable depth sets up a circulation pattern characterized by relatively strong barotropic coastal currents in the direction of the wind, with return flow occurring over the deeper regions. In a basin of the dimensions of Lake Ontario the effects of the Coriolis force on this forced flow pattern are relatively minor. Frictional effects are strong very close to the shores (within 7–9 km), but they do not modify qualitatively the flow pattern which may be simply calculated from the frictionless, linearized equations.

Acknowledgments. The theoretical work and data analysis were kindly supported by the IFYGL office of NOAA. The coastal chain field work was supported over several years by the Canada Centre for Inland Waters, and was carried out by a team under the supervision of B. Pade of the University of Waterloo.

REFERENCES

Bennett, J., 1972: On the dynamics of wind-driven lake currents. Ph.D. thesis, University of Wisconsin, Madison.

Birchfield, G. E., 1972: Theoretical aspects of wind-driven currents in a sea or lake of variable depth with no horizontal mixing. *J. Phys. Oceanogr.*, **2**, 355–352.

Csanady, G. T., 1972a: Response of large stratified lakes to wind. *J. Phys. Oceanogr.*, **2**, 3–13.

——, 1972b: The coastal boundary layer in Lake Ontario. *J. Phys. Oceanogr.*, **2**, 41–53; 168–176.

——, 1973: Transverse internal seiches in large, oblong lakes and marginal seas. W.H.O.I. Contrib. No. 3043.

——, and B. Pade, 1969–72: Coastal Jet Project Annual Reports. Environ. Fluid Mech. Lab., University of Waterloo, Ontario.

Heaps, N. S., 1969: A two-dimensional numerical sea model. *Phil. Trans. Roy. Soc. London*, **A265**, 93–137.

Paskausky, D. F., 1971: Winter circulation in Lake Ontario. *Proc. 14th Conf. Great Lakes Res.*, Rept. 593–606, Intern. Assoc. Great Lakes Res., Ann Arbor, Mich.

Rao, D. B., and T. S. Murthy, 1970: Calculation of the steady-state wind-driven circulation in Lake Ontario. *Arch. Meteor. Geophys. Bioklim.*, **A19**, 195–210.

Sweers, H. E., 1969: Structure, dynamics and chemistry of Lake Ontario. Marine Sciences Branch, Dept. Energy, Mines and Resources, Ottawa, 227 pp.

Wilson, B. W., 1972: Seiches. *Advances in Hydroscience*, V. T. Chow, Ed., Vol. 8, New York, Academic Press, 1–94.